

Luminescence of neutral and ionic gold(I) complexes containing pyrazole or pyrazolate-type ligands

Paloma Ovejero^a, María José Mayoral^a, Mercedes Cano^{a,*}, María Cristina Lagunas^b

^a Departamento de Química Inorgánica I, Facultad de Ciencias Químicas, Universidad Complutense, E-28040 Madrid, Spain

^b School of Chemistry and Chemical Engineering, Queen's University Belfast, Belfast BT9 5AG, UK

Received 30 November 2006; received in revised form 19 December 2006; accepted 19 December 2006

Available online 5 January 2007

Abstract

A series of pyrazole (Hpz) and pyrazolate (pz⁻) Au(I) complexes of types [Au(Hpz^{2R(n)})(PPh₃)]⁺ (**I**), [Au(Hpz^{2R(n)})₂]⁺ (**II**), [Au(μ-pz^{R(n)})₃] (**III**), [Au(pz^{R(n)/2R(n)})(PPh₃)] (**IV**), [AuCl(Hpz^{R(n)/2R(n)})] (**V**) and [(PPh₃)Au(μ-pz^{R(n)})Au(PPh₃)]⁺ (**VI**), R(*n*) and 2R(*n*) represent C₆H₄OC_nH_{2n+1} substituents at the 3- or 3- and 5-positions of the heterocyclic ring, respectively, have been shown to be luminescent in the solid state at 77 K, independently of the presence or not of inter-metallic Au–Au interactions. The emission spectra of all complexes consist of structured bands in the region 395–500 nm, attributed to ligand-to-metal charge transfer (LMCT) transitions involving the Hpz or pz⁻ ligands, the pattern of bands of compounds being related with the molecular structure and/or the nature of the ligands. The thermal behaviour of several complexes of the types **III**, **IV** and **V** containing long-chain substituents (*n* ≥ 12) was examined by polarising light optical microscopy (POM). The derivative [AuCl(Hpz^{R(12)})] was proved to have liquid crystal properties exhibiting a mesophase SmA but the remaining complexes were not liquid crystal materials. This complex is one of the scarce examples of Au(I) derivatives exhibiting both liquid crystal and luminescent properties.

© 2007 Elsevier B.V. All rights reserved.

Keywords: Gold(I) complexes; Pyrazole and pyrazolate ligands; Luminescence; Liquid crystal; Au–Au interactions

1. Introduction

Gold (I) complexes with neutral N-donor ligands are much less common than those with P-donor ligands because of the soft character of the metal centre [1]. However, our recent studies on the chemistry of substituted pyrazole-based complexes [2–6] have allowed us to describe compounds of the types [Au(Hpz^{2R(n)})(PPh₃)]⁺ (**I**), [Au(Hpz^{2R(n)})₂]⁺ (**II**), [Au(μ-pz^{R(n)})₃] (**III**) and [Au(pz^{R(n)/2R(n)})(PPh₃)] (**IV**) in which the pyrazole or pyrazolate groups carried R(*n*) substituents (R(*n*) = C₆H₄OC_nH_{2n+1}) at the 3- (Hpz^{R(n)}) or 3- and 5- (Hpz^{2R(n)}) positions of the heterocyclic ring. The X-ray crystal structures of representative examples of each family have been previously reported [2–6] and they are now revised in order to clarify if the

luminescent behaviour can be related to the presence of aurophilic interactions. In all the studied structures the Au centres exhibited the characteristic linear coordination, however only those of complexes of classes **III** and **IV** have shown short Au–Au contacts which were intra- or inter-molecular, respectively. By contrast, the structures of the cationic derivatives of classes **I** and **II** do not exhibit aurophilic interactions.

In this context it is interesting to note that luminescent properties of the linear Au(I) complexes are usually related to the presence of Au–Au interactions of less than 3.6 Å [5,7–16]. In fact, photoluminescence studies of complexes of the type [AuY₂]⁻, where Y represents an anionic ligand, have been used to elucidate the extension of inter-molecular Au–Au interactions [16]. Thus, cyanurate derivatives isolated as K⁺, Cs⁺, Tl⁺ salts exhibiting Au–Au contacts of 3.1–3.64 Å were proved to have luminescent properties, however those containing bulkier cations such as NBU₄⁺ in

* Corresponding author. Fax: +34 91 3944352.

E-mail address: mmcano@quim.ucm.es (M. Cano).

which the inter-molecular contacts were prevented behaved as not luminescent materials [16].

On the other hand, several di and polynuclear pyrazolate Au(I) complexes exhibiting luminescent behaviour have been reported [5,9–12,14]. In particular, for trimetallic derivatives of the type $[\text{Au}(\mu\text{-pz})_3]$ [11,12], the presence of Au–Au inter-molecular interactions has been considered responsible for the emissions whereas no luminescence was observed in analogous trigold species exhibiting only intra-molecular contacts [11]. The related digold(I) complexes of the types $[\text{Au}(\text{pz})(\text{PPh}_3)_2]$ [5,9] and $[\text{Au}_2(\mu\text{-pz})(\text{L}_2)]$ ($\text{L}_2 = (\text{PPh}_3)_2$, 1,3-diphenylphosphinopropane) [9], both exhibiting Au–Au contacts, give rise to structured emissions, which were attributed to ligand-to-metal charge transfer (LMCT) transitions. Luminescent tetrametallic species $[\text{Au}(\mu\text{-pz})_4]$ have also been described, and their emission attributed mainly to the presence of intra-molecular Au–Au contacts [14].

As it can be observed the luminescence properties of pyrazolate Au(I) complexes have been extensively explored in contrast to those of related pyrazole derivatives. However, several types of pyrazole Au(I) compounds have been described and structurally characterised [2,3].

In this context we decided to undertake a study of the structural and optical properties of several derivatives containing pyrazolate or pyrazole ligands. This comprises the investigation of the luminescence properties of cationic or neutral complexes of classes I–IV (1–11) [2,6], as well as those of the new derivatives of class V $[\text{AuCl}(\text{Hpz}^{\text{R}(n)})]$ (12) and $[\text{AuCl}(\text{Hpz}^{2\text{R}(n)})]$ (13, 14) and of class VI $[(\text{Ph}_3\text{P})\text{Au}(\mu\text{-pz}^{\text{R}(m)})\text{Au}(\text{PPh}_3)]^+$ (15) (Table 1).

The photoluminescence behaviour of complexes 1–15 (Table 1) is analysed taking into account the nature of the ligands, counterions (for the ionic derivatives) as well as the observed molecular structures, and related to the presence of inter-metallic interactions. To these effects the main results of the crystal structure of the new complex 15 are also presented.

In addition, following our previous experience in the design of liquid crystalline metal complexes based on mesogenic or pro-mesogenic R(n)-mono and disubstituted pyrazole ligands ($\text{R}(n) = \text{C}_6\text{H}_4\text{OC}_n\text{H}_{2n+1}$) [17–19], the complexes 6, 7, 11, 12 and 14 were considered as candidates to present liquid crystal properties and therefore very interesting as potential materials exhibiting both liquid crystal and luminescent properties. A study on their thermal properties is now presented.

2. Experimental

2.1. Materials and physical measurements

All commercial reagents were used as supplied. The starting Au-complexes $[\text{Au}(\text{NO}_3)(\text{PPh}_3)]$, $[\text{AuCl}(\text{tht})]$ (tht = tetrahydrothiophene), $[\text{Au}(\text{Tf})(\text{PPh}_3)]$ (Tf = CF_3SO_3), and the 3-substituted and 3,5-disubstituted pyrazoles, 3-[4-(alkyloxy)phenyl]-1H-pyrazoles ($\text{Hpz}^{\text{R}(n)}$) and 3,5-bis[4-

(alkyloxy)phenyl]-1H-pyrazoles ($\text{Hpz}^{2\text{R}(n)}$) were prepared by procedures described in previous works [17–20].

Elemental analyses for carbon, hydrogen, nitrogen were carried out by the Microanalytical Service of Complutense University. IR spectra were recorded on a FTIR ThermoNicolet 200 or on FTIR Nicolet Magna-550 spectrophotometers with samples as KBr pellets in the 4000–400 cm^{-1} region: vs (very strong), m (medium).

^1H NMR spectra were performed on a Bruker AC200 (200.13 MHz) and $^{31}\text{P}\{^1\text{H}\}$ NMR spectrum was recorded on a Bruker DPX-300 (121.49 MHz) of the NMR Service of Complutense University from solutions in CDCl_3 at room temperature. Chemical shifts $\delta(\text{H})$ (± 0.01 ppm) are listed relative to TMS using the signal of the deuterated solvent as reference (7.26 ppm), and $\delta(\text{P})$ (± 0.3 ppm) relative to 85% H_3PO_4 . Coupling constants (J) are in Hz (± 0.3 Hz). Multiplicities are indicated as s (singlet), d (doublet), t (triplet), m (multiplet), br (broad signal).

The electronic absorption spectra were recorded on a Perkin–Elmer UV/Vis spectrometer Lambda800. The emission spectra were recorded on a Perkin–Elmer LS55 luminescence spectrometer equipped with a R928 photomultiplier and a low temperature accessory.

Phase studies were carried out by optical microscopy using an Olympus BX50 microscope equipped with a Linkam THMS 600 heating stage. The temperatures were assigned on the basis of optic observations with polarised light.

2.2. Preparation of compounds 1–4 (types I and II)

The complexes 1–4 were synthesised as previously reported [2,3].

2.3. Preparation of compounds 5–7 (type III)

Complex 5 was prepared following our previously described method for compounds of the type $[\text{Au}(\mu\text{-pz}^{\text{R}(m)})_3]$ [6]. Analogous procedures were used to obtain the new derivatives 6 and 7, as described below.

2.3.1. Preparation of $[\text{Au}(\mu\text{-pz}^{\text{R}(14)})]_3$ (6)

Complex 6 was obtained as described previously [6] from $[\text{AuCl}(\text{tht})]$ (85.6 mg, 0.240 mmol), $\text{Hpz}^{\text{R}(14)}$ (77.0 mg, 0.240 mmol) and an excess of 60% NaH.

Yield: 56%. Elemental analyses: found: C 49.7, H 6.0, N 5.1%; calculated for $\text{C}_{69}\text{H}_{105}\text{N}_6\text{O}_3\text{Au}_3$: C 50.0, H 6.4, N 5.1. IR (KBr, cm^{-1}): 1612m $\nu(\text{C}=\text{N})$ + $\nu(\text{C}=\text{C})$. ^1H NMR (300 MHz, CDCl_3 , δ in ppm, J in Hz, 298 K): $\delta = 0.88$ (t, $^3J_{\text{H,H}} = 6.1$, CH_3), 1.77–1.82 (m, CH_2), 3.88 (t, $^3J_{\text{H,H}} = 6.6$, OCH_2), 4.01 (t, $^3J_{\text{H,H}} = 6.6$, OCH_2), 6.52 (d, $^3J_{\text{H,H}} = 2.2$, H-C(4)(pz)), 6.61 (d, $^3J_{\text{H,H}} = 8.5$, $\text{H}_{\text{meta}}(\text{C}_6\text{H}_4)$), 6.91 (d, $^3J_{\text{H,H}} = 2.2$, H-C(4)(pz)), 6.94 (d, $^3J_{\text{H,H}} = 8.5$, $\text{H}_{\text{meta}}(\text{C}_6\text{H}_4)$), 6.95 (d, $^3J_{\text{H,H}} = 2.2$, H-C(4)(pz)), 7.40 (d, $^3J_{\text{H,H}} = 2.2$, H-C(5)(pz)), 7.41 (d, $^3J_{\text{H,H}} = 2.2$, H-C(5)(pz)), 7.62 (d, $^3J_{\text{H,H}} = 8.0$, $\text{H}_{\text{ortho}}(\text{C}_6\text{H}_4)$), 7.90 (d, $^3J_{\text{H,H}} = 8.0$, $\text{H}_{\text{ortho}}(\text{C}_6\text{H}_4)$).

Table 1
Emission and excitation maxima (λ in nm) measured for complexes **1–15** in solid state at 77 K

Type	Counterion ^a	Substitution on pyrazole ring: 2R(<i>n</i>)=3,5-disubstituted, R(<i>n</i>)=3-substituted	Number of carbon atoms of the R(<i>n</i>) substituent: R(<i>n</i>) = C ₆ H ₄ OC _n H _{2n+1}	Number of compounds	λ_{exc}	λ_{em}^b
I [Au(Hpz ^{2R(<i>n</i>)})(PPh ₃) ⁺	NO ₃	2R(<i>n</i>)	<i>n</i> = 4	1	325	445, 474, 500
	PTS	2R(<i>n</i>)	<i>n</i> = 4	2	325	447, 470, 500
II [Au(Hpz ^{2R(<i>n</i>)}) ₂] ⁺	NO ₃	2R(<i>n</i>)	<i>n</i> = 4	3	330	445, 475, 500
	PTS	2R(<i>n</i>)	<i>n</i> = 4	4	330	447, 471, 500
III [Au(μ -pz ^{R(<i>n</i>)}) ₃	R(<i>n</i>)	R(<i>n</i>)	<i>n</i> = 4	5	315	434, 461, 488
	R(<i>n</i>)	R(<i>n</i>)	<i>n</i> = 14	6	315	435, 465, 493
	R(<i>n</i>)	R(<i>n</i>)	<i>n</i> = 16	7	315	436, 463, 495
IV [Au(pz ^{2R(<i>n</i>)})(PPh ₃)] [Au(pz ^{R(<i>n</i>)})(PPh ₃)]	2R(<i>n</i>)	2R(<i>n</i>)	<i>n</i> = 4	8	320	415, 445, 470 ^c
	2R(<i>n</i>)	2R(<i>n</i>)	<i>n</i> = 6	9	337	428, 446, 482 ^c
	2R(<i>n</i>)	2R(<i>n</i>)	<i>n</i> = 8	10	321	419, 446, 482 ^c
	R(<i>n</i>)	R(<i>n</i>)	<i>n</i> = 14	11	315	421, 446, 467
V [AuCl(Hpz ^{R(<i>n</i>)})] [AuCl(Hpz ^{2R(<i>n</i>)})]	R(<i>n</i>)	R(<i>n</i>)	<i>n</i> = 12	12	315	396, 416, 435
	2R(<i>n</i>)	2R(<i>n</i>)	<i>n</i> = 4	13	315	395, 416, 439
	2R(<i>n</i>)	2R(<i>n</i>)	<i>n</i> = 12	14	315	395, 417, 436
VI [(PPh ₃)Au(μ -pz ^{R(<i>n</i>)}) Au(PPh ₃)] ⁺	Tf	R(<i>n</i>)	<i>n</i> = 8	15	300	429, 458, 482

^a PTS = *p*-toluenesulfonate (CH₃-*p*-C₆H₄SO₃); Tf = trifluoromethanesulfonate (CF₃SO₃).

^b λ_{em} in bold means the most intense band.

^c Reference [5].

2.3.2. Preparation of [Au(μ -pz^{R(16)})]₃ (**7**)

Complex **7** was synthesised as described [6] from [AuCl(tht)] (100 mg, 0.202 mmol), Hpz^{R(16)} (77.7 mg, 0.202 mmol) and an excess of 60% NaH.

Yield: 41%. Elemental analyses: found: C 51.3, H 6.6, N 4.7%; calculated for C₇₅H₁₁₇N₆O₃Au₃: C 51.7, H 6.8, N 4.8. IR (KBr, cm⁻¹): 1612m ν (C=N) + ν (C=C). ¹H NMR (300 MHz, CDCl₃, δ in ppm, *J* in Hz, 298 K): δ = 0.88 (t, ³J_{H,H} = 6.7, CH₃), 1.76–1.85 (m, CH₂), 3.88 (t, ³J_{H,H} = 6.6, OCH₂), 4.03 (t, ³J_{H,H} = 6.6, OCH₂), 6.57 (d, ³J_{H,H} = 2.4, H-C(4)(pz)), 6.60 (d, ³J_{H,H} = 2.4, H-C(4)(pz)), 6.64 (d, ³J_{H,H} = 8.3, H_{meta}(C₆H₄)), 6.65 (d, ³J_{H,H} = 2.4, H-C(4)(pz)), 6.97 (d, ³J_{H,H} = 8.3, H_{meta}(C₆H₄)), 7.39 (d, ³J_{H,H} = 2.2, H-C(5)(pz)), 7.51 (d, ³J_{H,H} = 2.2, H-C(5)(pz)), 7.65 (d, ³J_{H,H} = 8.8, H_{ortho}(C₆H₄)), 7.92 (d, ³J_{H,H} = 8.8, H_{ortho}(C₆H₄)).

2.4. Preparation of compounds **8–11** (type **IV**)

The compounds **8–10** were synthesised as reported by us in a previous work [5]. A similar method was used to obtain **11**, as indicated below.

2.4.1. Preparation of [Au(pz^{R(14)})(PPh₃)₂] (**11**)

Complex **11** was prepared as described [5] from [Au(NO₃)(PPh₃)] (44 mg, 0.084 mmol) and Napz^{R(14)}. The latter was obtained in situ from Hpz^{R(14)} (30.7 mg, 0.084 mmol) and an excess of 60% NaH.

Yield: 60%. Elemental analyses: found: C 60.1, H 6.0, N 3.4%; calculated for C₈₂H₁₀₀N₄O₂P₂Au₂: C 60.4, H 6.2, N 3.4%. IR (KBr, cm⁻¹): 1613m ν (C=N) + ν (C=C). ¹H NMR (300 MHz, CDCl₃, δ in ppm, *J* in Hz, 298 K): δ = 0.71 (t, ³J_{H,H} = 6.6, CH₃), 1.62 (m, CH₂), 3.80 (t, ³J_{H,H} = 6.6, OCH₂), 6.5 (br, H-C(4)(pz)), 6.72 (d, ³J_{H,H} = 8.6, H_{meta}(C₆H₄)), 7.34 (br, H-C(5)(pz)), 7.63 (d, ³J_{H,H} = 8.6, H_{ortho}(C₆H₄)). ³¹P{¹H} NMR (121.49 MHz, CDCl₃, δ in ppm, 298 K): δ = 32.8.

2.5. Preparation of complexes **12–14** (type **V**)

2.5.1. Preparation of [AuCl(Hpz^{R(12)})] (**12**)

A THF solution (20 mL) of Hpz^{R(12)} (90 mg, 0.274 mmol) was added to a solution of [AuCl(tht)] (87.9 mg, 0.274 mmol) in dry THF (20 mL). After 24 h of stirring, the resulting mixture was filtered through a plug of Celite and the colourless filtrate was evaporated to dryness. The residue was dissolved in CH₂Cl₂ and precipitated with hexane.

Yield: 40%. Elemental analyses: found: C 44.6, H 5.6, N 4.9%; calculated for C₂₁H₃₂ClN₂OAu: C 45.0, H 5.7, N 5.0. IR (KBr, cm⁻¹): 3198m ν (NH), 1615vs ν (C=N) + ν (C=C). ¹H NMR (300 MHz, CDCl₃, δ in ppm, *J* in Hz, 298 K): δ = 0.90 (t, ³J_{H,H} = 6.7, CH₃), 1.20–1.70 (m, CH₂), 1.83 (m, CH₂), 4.03 (t, ³J_{H,H} = 6.4, OCH₂), 6.61 (s, H-C(4)(pz)), 6.99 (d, ³J_{H,H} = 8.6, H_{meta}(C₆H₄)), 7.39 (s, H-C(5)(pz)), 7.45 (d, ³J_{H,H} = 8.6, H_{ortho}(C₆H₄)), 12.54 (s, NH).

2.5.2. Preparation of $[AuCl(Hpz^{2R(4)})]$ (**13**)

As described for **12**, from $Hpz^{2R(4)}$ (85.1 mg, 0.223 mmol) and $[AuCl(tht)]$ (74.9 mg, 0.233 mmol).

Yield: 52%. Elemental analyses: found: C 46.4, H 5.1, N 4.5%; calculated for $C_{23}H_{28}ClN_2O_2Au$: C 46.3, H 4.7, N 4.7. IR (KBr, cm^{-1}): 3234m $\nu(NH)$, 1615vs $\nu(C=N) + \nu(C=C)$. 1H NMR (300 MHz, $CDCl_3$, δ in ppm, J in Hz, 298 K): $\delta = 0.85$ (t, $^3J_{H,H} = 6.1$, CH_3), 1.11–1.72 (m, CH_2), 3.86 (t, $^3J_{H,H} = 6.4$, OCH_2), 6.54 (s, H-C(4)(pz)), 6.81 (d, $^3J_{H,H} = 8.6$, $H_{meta}(C_6H_4)$), 7.49 (d, $^3J_{H,H} = 8.6$, $H_{ortho}(C_6H_4)$).

2.5.3. Preparation of $[AuCl(Hpz^{2R(12)})]$ (**14**)

As described for **12**, from $Hpz^{2R(12)}$ (105.9 mg, 0.181 mmol) and $[AuCl(tht)]$ (58.0 mg, 0.181 mmol).

Yield: 45%. Elemental analyses: found: C 57.0, H 7.4, N 3.3%; calculated for $C_{39}H_{60}ClN_2O_2Au$: 57.0, H 7.4, N 3.4%. IR (KBr, cm^{-1}): 3430m $\nu(NH)$, 1615vs $\nu(C=N) + \nu(C=C)$. 1H NMR (300 MHz, $CDCl_3$, δ in ppm, J in Hz, 298 K): $\delta = 0.88$ (t, $^3J_{H,H} = 5.6$, CH_3), 1.74–1.87 (m, CH_2), 3.99 (t, $^3J_{H,H} = 6.0$, OCH_2), 6.69 (s, H-C(4)(pz)), 6.95 (d, $^3J_{H,H} = 8.8$, $H_{meta}(C_6H_4)$), 7.64 (d, $^3J_{H,H} = 8.8$, $H_{ortho}(C_6H_4)$).

2.6. Preparation of $[(Ph_3P)Au(\mu-pz^{R(8)})Au(PPh_3)]Tf$ (**15**) (type VI)

To a solution of $[Au(Tf)(PPh_3)]$ (60 mg, 0.098 mmol) in 25 mL of dry THF was slowly added $Napz^{R(8)}$, prepared by treating $Hpz^{R(8)}$ (13.32 mg, 0.049 mmol) with an excess of 60% NaH in dry THF. The mixture was stirred for 24 h, then filtered through Celite. The filtrate was evaporated to dryness and the residue was dissolved in CH_2Cl_2 . Upon addition of hexane, a white precipitate formed, which was filtered and dried in vacuo. Crystals were obtained by slow diffusion of hexane into a CH_2Cl_2 solution of **15**.

Yield: 60%. Elemental analyses: found: C 48.2, H 4.0, N 2.1%; calculated for $C_{54}H_{53}F_3N_2O_4P_2SAu_2$: C 48.4, H 4.0, N 2.1. IR (KBr, cm^{-1}): 1611vs $\nu(C=N) + \nu(C=C)$. 1H NMR (300 MHz, $CDCl_3$, δ in ppm, J in Hz, 298 K): $\delta = 0.88$ (t, $^3J_{H,H} = 6.1$, CH_3), 1.11–1.72 (m, CH_2), 3.86 (t, $^3J_{H,H} = 6.4$, OCH_2), 6.85 (d, $^3J_{H,H} = 8.6$, $H_{meta}(C_6H_4 + H-C(4)(pz))$), 7.49 (d, $^3J_{H,H} = 8.6$, $H_{ortho}(C_6H_4) + H-C(5)(pz)$). $^{31}P\{^1H\}$ NMR (121.49 MHz, $CDCl_3$, δ in ppm, 298 K): $\delta = 32.1$.

3. Results and discussion

3.1. Spectroscopic and structural characterisation

Typical structures for each class of compounds are established on the basis of a single crystal X-ray data of representative examples described in previous works [2,6] and in this work (Fig. 1b). Fig. 1a depicts a schematic representation of molecular structures for the complexes of classes I–VI.

The analytical and spectroscopic data of the new complexes (Section 2) are in agreement with the proposed formulation. Selected spectroscopic and structural features are discussed below.

The new complexes of the families III (**6, 7**) and IV (**11**) containing long-chain R(*n*)-substituents ($n \geq 14$) on the pyrazole have been synthesised by a procedure similar to that described for related complexes [5,6].

The 1H NMR data for new trinuclear pyrazolate complexes (type III) $[Au(\mu-pz^{R(14)})]_3$ (**6**) and $[Au(\mu-pz^{R(16)})]_3$ (**7**) indicate the presence of an asymmetric trimetallic unit. Thus, the spectra exhibit three H-C(4) and two H-C(5) signals in a 1:1:1 and 2:1 ratio, respectively, in agreement with the presence of non-equivalent pyrazolate groups. Accordingly, a similar pattern is observed for the OCH_2 and aromatic protons of the R substituents. The latter appear as two doublets ($^3J_{H,H} \approx 8$ Hz) for each the *ortho* and *meta* protons at ca. 7.6 and 7.9 ppm, and 6.6 and 6.9 ppm, respectively, whereas the OCH_2 groups give two triplets ($^3J_{H,H} \approx 6.6$ Hz) at ca. 3.9 and 4.0 ppm, in a 4:2 ratio.

In the absence of adequate crystals of **6** and **7** for X-ray structural determination, the structure of these compounds has been considered similar to that found for the related complex $[Au(\mu-pz^{2PP})]_3(pz^{2PP} = 3,5\text{-bis(4-phenoxyphe-nyl)pyrazolate})$ (**16**) [6] (Fig. 1b), which shows a trigonal geometry in which the three metal centres are connected through intra-molecular Au–Au contacts of 3.309(1) Å [6].

The 1H NMR spectrum of complex **11** exhibits the characteristic signals of monosubstituted pyrazole ligand. All attempts to get adequate crystals for X-ray structural determination of this complex were unsuccessful and then the X-ray crystal structure of the related compound (**8**) [4] was used as reference (Fig. 1b). The molecular structure of the later shows a dimeric nature in which the individual molecules are connected through inter-molecular Au–Au contacts of 3.029(1) Å.

The compounds **12**, **13**, **14** (type V) and **15** (type VI) involved new structural types to respect to those previously described.

Type V complexes $[AuCl(Hpz^{R(12)})]$ (**12**), $[AuCl(Hpz^{2R(4)})]$ (**13**) and $[AuCl(Hpz^{2R(12)})]$ (**14**) were prepared from equimolecular reactions between $[AuCl(tht)]$ and the corresponding pyrazole ligand. The pyrazole ligands, $Hpz^{R(12)}$, $Hpz^{2R(4)}$ and $Hpz^{2R(12)}$, were selected to study the influence of the alkyl chain length as well as the effect of mono- versus di-substitution of the pyrazole ring on the luminescence properties of the complexes.

In addition, the thermal behaviour of the new complexes **12** and **14** with potential for liquid crystal properties was also examined and the results will be discussed below.

The type VI complex, **15**, was prepared by reaction of $[Au(Tf)(PPh_3)]$ [17] and $Napz^{R(8)}$ in a 2:1 molar ratio. The crystal structure of **15** was determined by X-ray diffraction and we describe here only the results conducting to show the presence of metal–metal interactions. The

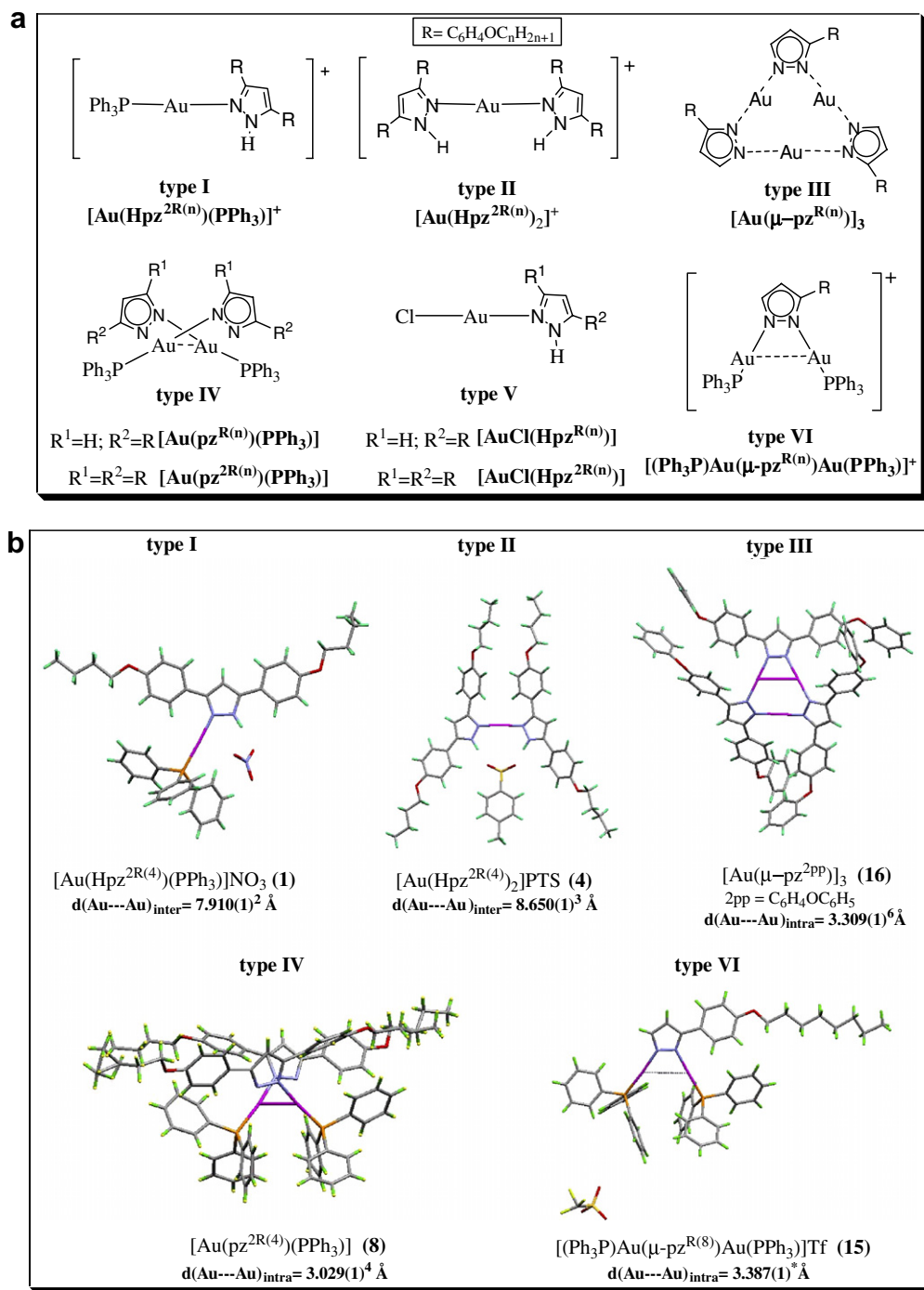


Fig. 1. (a) Schematic representation of molecular structures for the complexes of types I–VI and (b) crystal structures of classes I–IV and VI.

molecular structure (Fig. 1b) consists of one bimetallic unit in which each Au(I) centre is coordinated to a PPh₃ ligand and N-bonded to a bridging pyrazolate ligand. The coordination around each metal is almost linear (177.87°) and the two Au(I) atoms in the molecule are separated by 3.387(1) Å, in agreement with a weak intra-molecular Au–Au interaction. Full structural data will be published as part of a comparative study of Au–pyrazolate complexes, which is currently in progress.

The crystal structures of complexes [Au(Hpz^{2R(4)})(PPh₃)]NO₃ (**1**) and [Au(Hpz^{2R(4)})₂]PTS (**4**) (PTS = CH₃-*p*-C₆H₄SO₃) and [Au(pz^{R(4)})(PPh₃)] (**8**), from classes I, II and IV, respectively, are included in Fig. 1b, to aid the discussion of the optical results. Compounds **1** and **4** (Fig. 1b) show monomeric structures in which neither inter- nor intra-molecular Au–Au contacts were found [2,3], however, the complex **8** (Fig. 1b) forms dimers in the solid state through strong Au–Au interactions of 3.029(1) Å [4].

3.2. Thermal studies

The complexes **6**, **7**, **11**, **12** and **14** having long chain substituent on the pyrazole ring were studied by optical microscopy under polarized light (POM). Differential scanning calorimetry (DSC) was used for those complexes exhibiting liquid crystalline behaviour.

In previous works, we have shown that both 3-mono-substituted ($\text{Hpz}^{\text{R}(n)}$) and 3,5-disubstituted ($\text{Hpz}^{2\text{R}(n)}$) pyrazoles containing alkyloxyphenyl substituents $\text{C}_6\text{H}_4\text{O}-\text{C}_n\text{H}_{2n+1}$ can induce mesomorphism upon coordination to different metal fragments. However, only the disubstituted pyrazole ($\text{Hpz}^{2\text{R}(n)}$) ($n=4-18$ carbon atoms) presents liquid crystal properties as free ligands [17–19], in contrast with the non-mesogenic behaviour of the related monosubstituted $\text{Hpz}^{\text{R}(n)}$ ligands. In view of these results, we undertook the study of the thermal behaviour of selected compounds of types **III**, **IV** and **V** with $n \geq 12$.

The trimeric complexes of class **III** (**6**, **7**) were proposed as adequate candidates for liquid crystal properties. In fact, the related complex $[\text{Au}(\mu\text{-pz}^{\text{R}(n)})]_3$ ($n=12$) had been proved to have columnar mesophases consistent with the columnar distribution of disc-like non-planar trimers observed in the X-ray structure of **16** [6]. However, those with shorter ($n=4$) or longer ($n=18$) chains behaved as non-liquid crystal materials [6].

POM observations of complexes **6** and **7** having 14 and 16 carbon atoms in the alkylic chains showed that the complexes were non-mesomorphic and simply melted to the isotropic state. It appears that the increase to 14, 16 or 18 carbon atoms in the alkylic chains disrupts the ordering on the columnar arrangement of mesophases established for the complex with 12 carbon atoms.

Quite interestingly the coordination of the non-mesogenic $\text{Hpz}^{\text{R}(12)}$ as pyrazolate ligand to the AuCl fragment (complex **12**) results in the appearance of a mesomorphic behaviour which was monotropic. So after the phase transition from solid to the isotropic liquid at 82.4 °C, the mesophase was observed on cooling (Fig. 2) at 69.2 °C exhibiting an oily streak texture characteristic of SmA mesophases. Crystallization begins to take place close to the temperature of formation of mesophase. As a consequence only a broad peak, attributed to an overlapping of both phase transitions I-SmA and SmA-Cr, could be observed on the thermogram of DSC. In agreement with that consideration the enthalpy value ($\Delta H = -39.49 \text{ kJ mol}^{-1}$) was high enough to involve both sequential and overlapped processes (Fig. 3).

Subsequent DSC scans show on heating a behaviour analogous to that observed on the first cycle. However, on the second cooling the thermogram exhibits an additional peak at 52.2 °C that should correspond to the crystallization process from the mesophase as it had also been observed under MOP. The mesophase was then stable between 65 and 52 °C.

Complex $[\text{AuCl}(\text{Hpz}^{2\text{R}(12)})]$ (**14**) did not exhibit mesomorphic properties. It is solid at room temperature and

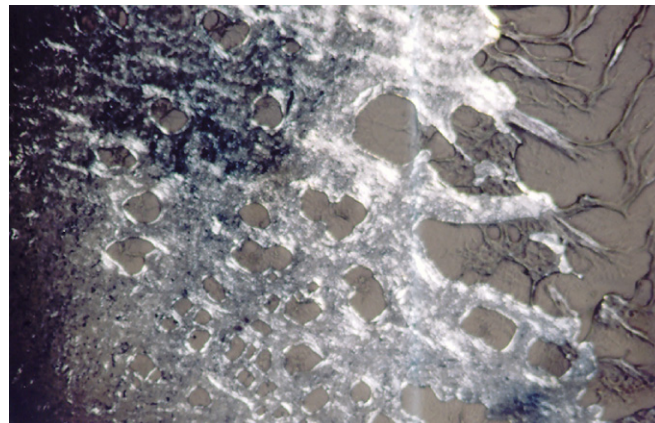


Fig. 2. Texture of the SmA mesophase on second cooling of $[\text{AuCl}(\text{Hpz}^{\text{R}(12)})]$ (**12**) at 60 °C.

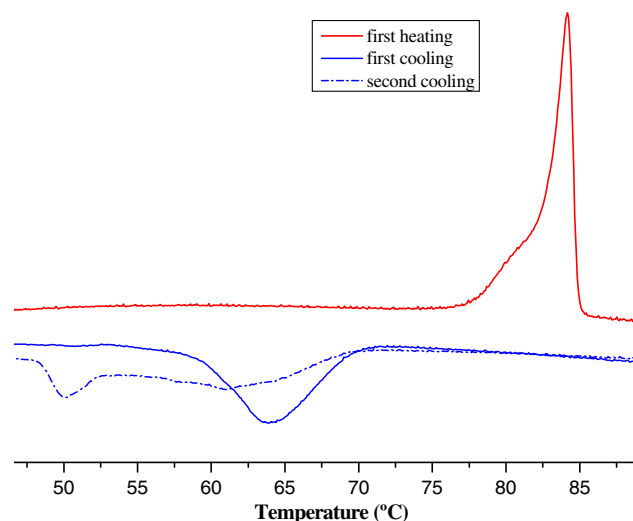


Fig. 3. DSC thermogram of $[\text{AuCl}(\text{Hpz}^{\text{R}(12)})]$ (**12**).

melts at 155 °C to the isotropic liquid. Upon cooling a single phase transition corresponding to the crystallization from the isotropic liquid was observed.

The different thermal behaviour of **12** and **14** can be explained by considering the more appropriate molecular shape of complex **12**, compared to that of **14** for liquid crystal properties. The former, containing a sole R substituent at the 3-position of the pyrazole ring, could form a rod-like elongated dimeric structure, such as that depicted in Fig. 4, which would be responsible for the smectic mesophase observed. That structure should not be possible for the related compound **14** with 3,5-disubstituted pyrazole.

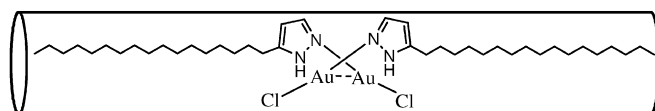


Fig. 4. Schematic representation of $[\text{AuCl}(\text{Hpz}^{\text{R}(12)})]$ (**12**) in which the rod-like elongated dimeric structure is visualised.

Unfortunately, all attempts to get crystals of type V complexes suitable for X-ray diffraction studies were unsuccessful, that feature being commonly found for complexes based on long chained pyrazole ligands.

None of type IV complexes exhibited mesomorphism, which should be expected on the basis of their molecular shape containing the bulky PPh_3 ligand.

3.3. Luminescence studies

All compounds 1–15 are luminescent in the solid state at 77 K, and give rise to structured bands in the region 395–500 nm. The emission and excitation maxima are recovered in Table 1. Some of the complexes (1, 6, 11 and 14) also emit at room temperature, showing emission bands at similar energies that those at 77 K, but generally less resolved and of lower intensity.

The emission spectra at 77 K of the complexes exhibit two types of patterns of bands, namely A or B. Representative examples of these two types of emission pattern observed for 7 (type A) and 4 (type B) are shown in Fig. 5. They both consist on a three component emission band, with the component of higher intensity being the first one in B and the middle one in A.

Complexes containing pyrazolate ligands (classes III, IV and VI) give type A spectra, whereas those with pyrazole ligands (classes I, II and V) exhibit a type B pattern, independently of whether they are cationic or neutral. For complexes with type B spectra, however, the substitution of a neutral Hpz ligand by an anionic Cl ligand (compare compounds of classes II and V) results in a shift of the emission maxima to lower wavelengths, but no shift is observed when Hpz is exchanged by another neutral ligand, PPh_3 (compare compounds of classes II and I).

The presence of one or two chains on the pyrazole ligand does not significantly affect the emission (i.e., compare 12 and 14). The spectra are also unaffected by the

chain length of the $\text{R}(n)/2\text{R}(n)$ -substituents (compare 13–14, 8–10, or 5–7).

The room temperature solid-state emission of some of the free pyrazoles was also measured for comparison. The 3-substituted pyrazoles ($\text{Hpz}^{\text{R}(n)}$) showed an intense band at 320 nm when excited at 275 nm, whereas the 3,5-disubstituted ($\text{Hpz}^{2\text{R}(n)}$) emitted at 340 nm ($\lambda_{\text{exc}} = 290$ nm).

Taken the above observations into account, and given the similarity of all the solid-state emission spectra of the Au(I) compounds as well as their vibronic structures, the most plausible origin for the luminescence of the complexes is a ligand (Hpz/pz^-) to metal charge transfer (LMCT) transition [9,10]. The energy separation between the two first (and well-defined) emission maxima in the spectra ranges between 1100 and 1470 cm^{-1} , and corresponds well with $\nu(\text{C}=\text{C})$ and/or $\nu(\text{C}=\text{N})$ vibrations of the pyrazole/pyrazolate rings. However, given the presence of Au–Au contacts in the pyrazolate derivatives of the families III, IV and VI, some ligand-to-metal–metal charge transfer (LMMCT) character of the emission cannot be ruled out in these complexes.

As it can be deduced from our structural data (Fig. 1b) the complexes 8 and 15 whose emission pattern was analogous to that of all complexes of classes III, IV and VI (Table 1) exhibited short inter and intra Au–Au contacts of 3.029(1) and 3.387(1) Å, respectively. On the other hand for trimeric complexes of class III (5, 6 and 7) intra-molecular Au–Au contacts as those found on 16 can also be suggested.

In agreement with those results we should also consider that several trimetallic pyrazolate complexes exhibiting both intra- and inter-molecular Au–Au contacts have shown to give metal-centered emissions consisting of broad unstructured bands at 625–630 nm [11,21]. By contrast the complex $[\text{Au}(\mu\text{-3-Me-5-Ph-pz})_3]$, where inter-molecular contacts are prevented by bulky substituents on the pyrazolate rings, was not luminescent at room temperature [11].

On the other hand, pyrazolate phosphine complex of the type $[(\text{PPh}_3)_2\text{Au}(\mu\text{-3,5-Ph}_2\text{pz})]\text{NO}_3$ analogous to those of classes IV and VI [9] have shown similar spectra to those described here. The presence of Au–Au interactions not being solely responsible for the observed emission.

In summary, despite their structural variety, the luminescence of complexes 1–15 appears to be mainly dominated by the Hpz/pz^- ligands, with the emissive states perturbed by their coordination to the gold atoms but not determined by the presence of Au–Au interactions.

The different spectra observed for complexes of classes III, IV and VI, containing Au–Au contacts, compared to those of compounds of types I and II, without Au–Au interactions, could be related not only to the different nature of the ligands, but also to the presence of the interactions. Similarly, and given that the presence of Au–Au contacts in type V complexes cannot be ruled out, the shift observed in the emission of these compounds, compared to that of I or II, could be partly attributed to those interactions.

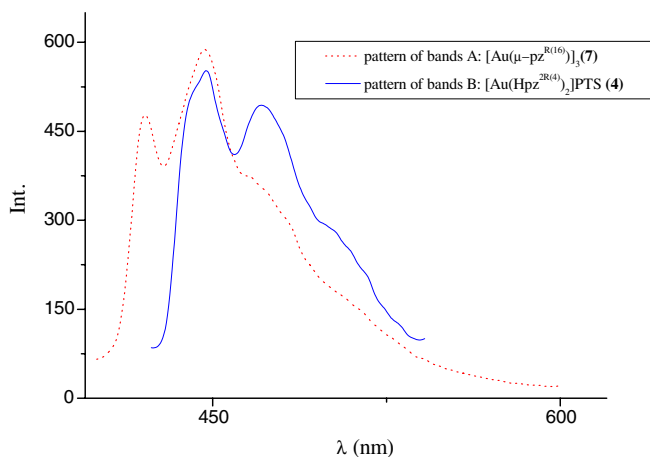


Fig. 5. Emission spectra of the two types of pattern of bands A or B.

4. Conclusions

This paper has shown the use of pyrazolate or pyrazole ligands bonded to Au(I) metal centres or AuL metal fragments ($L = \text{Cl}, \text{PPh}_3, \text{Hpz}$) in the construction of luminescent materials.

All complexes investigated exhibit luminescence at 77 K in solid state but not all of them have shown to have Au–Au interactions on their structures. So the X-ray study of single crystals of the pyrazolate complexes **8**, **15** and **16** (Fig. 1b) from the types $[\text{Au}(\text{pz}^{2R(n)})(\text{PPh}_3)]$ (**IV**), $[(\text{PPh}_3)\text{-Au}(\mu\text{-pz}^{2R(n)})\text{Au}(\text{PPh}_3)]^+$ (**VI**) and $[\text{Au}(\mu\text{-pz}^{2R(n)})]_3$ (**III**), respectively, indicated the presence of short Au–Au contacts which were absent in the structures of pyrazole based derivatives **1** and **4** from classes $[\text{Au}(\text{Hpz}^{2R(n)})(\text{PPh}_3)]^+$ (**I**) and $[\text{Au}(\text{Hpz}^{2R(n)})_2]^+$ (**II**).

The pattern of the emission bands on both pyrazolate (**III**, **IV** and **VI**) and pyrazole (**I**, **II** and **V**) based complexes was slightly different, in both cases corresponding with a three component structured emission band. Those differences could be related not only to the different nature of ligands (Hpz or pz^-) but the presence of Au–Au interactions. In summary, the luminescence of complexes **1–15** appears to be mainly dominated by the Hpz/pz^- ligands, with the emissive states perturbed by their coordination to the gold atoms but not determined by the presence of Au–Au interactions. The origin of the luminescence can be attributed to ligand-to-metal charge transfer (LMCT) transitions involving the Hpz or pz^- ligands or a ligand-to-metal–metal charge transfer (LMMCT) in those cases with Au–Au contacts.

Acknowledgements

We are grateful to the Dirección General de Investigación/MEC of Spain (Project No. BQU2003-07343) and The Royal Society (Project No.15076) for financial support. We also thank to Universidad Complutense of Madrid for the predoctoral fellowship to M.J.M.

References

- [1] J. Vicente, M.T. Chicote, I. Saura-Llamas, M.C. Lagunas, M.C. Ramírez de Arellano, P. González-Herrero, M.D. Abrisqueta, R.

- Guerrero, in: P. Braunstein, L.A. Oro, P.R. Raithby (Eds.), *Metal Clusters in Chemistry*, vol. 1, Wiley-VCH, Weinheim, 1999, p. 493.
- [2] R.M. Claramunt, P. Cornago, M. Cano, J.V. Heras, M.L. Gallego, E. Pinilla, M.R. Torres, *Eur. J. Inorg. Chem.* (2003) 2693.
- [3] M.L. Gallego, P. Ovejero, M. Cano, J.V. Heras, J.A. Campo, E. Pinilla, M.R. Torres, *Eur. J. Inorg. Chem.* (2004) 3089.
- [4] P. Ovejero, M. Cano, E. Pinilla, M.R. Torres, *Helv. Chim. Acta* 85 (2002) 1686.
- [5] P. Ovejero, M. Cano, J.A. Campo, J.V. Heras, A. Laguna, O. Crespo, E. Pinilla, M.R. Torres, *Helv. Chim. Acta* 87 (2004) 2057.
- [6] M.C. Torralba, P. Ovejero, M.J. Mayoral, M. Cano, J.A. Campo, J.V. Heras, E. Pinilla, M.R. Torres, *Helv. Chim. Acta* 87 (2004) 250.
- [7] E.J. Fernández, A. Laguna, J.M. López de Luzuriaga, *Gold Bull.* 34 (2001) 14.
- [8] E.J. Fernández, A. Laguna, J.M. López de Luzuriaga, *Anal. Quím.* 97 (2001) 34.
- [9] A.A. Mohamed, T. Grant, R.J. Staples, J.P. Fackler Jr., *Inorg. Chim. Acta* 357 (2004) 1761.
- [10] A.A. Mohamed, J.M. López-de-Luzuriaga, J.P. Fackler Jr., *J. Cluster Sci.* 14 (2003) 61.
- [11] G. Yang, R.G. Raptis, *Inorg. Chem.* 42 (2003) 261.
- [12] M.A. Omary, M.A. Rawashdeh-Omary, M.W. Alexander Gonser, O. Elbjeirami, T. Grimes, T.R. Cundari, H.V.K. Diyabalanage, C.S. Palehepitiya, H.V. Rasika Dias, *Inorg. Chem.* 44 (2005) 8200.
- [13] M.A. Rawashdeh-Omary, M.A. Omary, J.P. Fackler Jr., R. Galassi, B.R. Pietroni, A. Burini, *J. Am. Chem. Soc.* 123 (2001) 9689.
- [14] G. Yang, R.G. Raptis, *Inorg. Chim. Acta* 352 (2003) 98.
- [15] A. Burini, R. Bravi, J.P. Fackler Jr., R. Galassi, T.A. Grant, M.A. Omary, B.R. Pietroni, R.J. Staples, *Inorg. Chem.* 39 (2000) 3158.
- [16] Z. Assefa, B.G. McBurnett, R.J. Staples, J.P. Fackler Jr., B. Assmann, K. Angermaier, H. Schmidbaur, *Inorg. Chem.* 34 (1995) 75.
- [17] M.C. Torralba, M. Cano, J.A. Campo, J.V. Heras, E. Pinilla, M.R. Torres, *Inorg. Chem. Commun.* 5 (2002) 887; M. Cano, J.V. Heras, M. Maeso, M. Alvaro, R. Fernández, E. Pinilla, J.A. Campo, A. Monge, *J. Organomet. Chem.* 534 (1997) 159; M.C. Torralba, M. Cano, J.A. Campo, J.V. Heras, E. Pinilla, M.R. Torres, *J. Organomet. Chem.* 633 (2001) 91.
- [18] J. Barberá, C. Cativiela, J.L. Serrano, M.M. Zurbano, *Liq. Cryst.* 11 (1992) 887; M.C. Torralba, M. Cano, J.A. Campo, J.V. Heras, E. Pinilla, M.R. Torres, *J. Organomet. Chem.* 654 (2002) 150.
- [19] M.C. Torralba, M. Cano, S. Gómez, J.A. Campo, J.V. Heras, J. Perles, C. Ruiz-Valero, *J. Organomet. Chem.* 682 (2003) 26.
- [20] L. Malatesta, L. Naldini, G. Simonetta, F. Cariati, *Coord. Chem. Rev.* 1 (1966) 255; R. Usón, A. Laguna, M. Laguna, *Inorg. Synth.* 296 (1989) 85; M. Preisenberger, A. Schier, H. Schmidbaur, *J. Chem. Soc., Dalton Trans.* (1999) 1645.
- [21] H.V. Rasita Días, H.V.K. Diyabalanage, M.G. Eldabaja, O. Elbjeirami, M.A. Rawashdeh-Omary, M.A. Omary, *J. Am. Chem. Soc.* 127 (2005) 7489.